A EUROPEAN JOURNAL OF CHEMICAL BIOLOGY

CHEMBIOCHEM

SYNTHETIC BIOLOGY & BIO-NANOTECHNOLOGY

Accepted Article

Title: Cyano-modification on Uridine Decrease the Base Pairing Stability and Specificity through Neighbouring Disruption in RNA Duplex

Authors: Song Mao, Srivathsan V. Ranganathan, Hsu-Chun Tsai, Phensinee Haruehanroengra, Fusheng Shen, vibhav A Valsangkar, Bo Han, Abdalla E. A. Hassan, Alan Chen, and Jia Sheng

To be cited as: *ChemBioChem* 10.1002/cbic.201800399

Link to VoR: http://dx.doi.org/10.1002/cbic.201800399

A Journal of ChemPubSoc Europe

WILEY-VCH www.chembiochem.org

Cyano-modification on Uridine Decrease the Base Pairing Stability and Specificity through Neighbouring Disruption in RNA Duplex

Song Mao,[a] Srivathsan V. Ranganathan,[a] Hsu-Chun Tsai,[a] Phensinee Haruehanroengra,[a] Fusheng Shen,[a] Vibhav A. Valsangkar,[a] Bo Han,[a,b] Abdalla E. A. Hassan,[c] Alan Chen[a] and Jia Sheng*[a]

Abstract: 5-cyanomethyluridine (cnm^{5}U) and 5-cyanouridine (cn^{5}U), the two uridine analogues, were synthesized and incorporated into RNA oligonucleotides. The base pairing stability and specificity studies in RNA duplexes indicated that cnm^{5}U slightly decreases the duplex stability but retains the base pairing preference. In contrast, cn^{5}U dramatically decreases both base pairing stability and specificity between U:A and other non-canonical U:G, U:U and U:C pairs. In addition, the cn^{5}U:G pair is stronger than the cn^{5}U:A pair and the other mismatched pairs in the context of RNA duplex, implying the cn^{5}U might slightly prefer to recognize G over A. Our mechanistic studies by molecular simulation showed that the cn^{5}U modification does not directly affect the base-pairing of the parent nucleotide, instead, it weakens the neighbouring base-pair in the 5' side of the modification in the RNA duplexes. Consistent with the simulation data, replacing the Watson-Crick A:U pair to a mismatched C:U pair in the 5'-neighboring site does not affect the overall duplex stability. Our work implies the significance of electron-withdrawing cyano-group in natural tRNA systems and provides two novel building blocks for constructing RNA-based therapeutics.

Introduction

RNA plays essential and diverse roles in living systems as genetic information carrier, functional regulator and catalyst.[1-4] The structures and functions of RNA in cells are further diversified in the presence of various posttranscriptional chemical modifications. To date, more than 150 chemical modifications, which decorate different positions of nucleobase and ribose in RNA nucleotides, have been discovered in all the natural life domains.[5-7] These chemical modifications could mediate and fine-tune many specific base pairing patterns,[8] which are critical for RNA to fold into well-defined functional structures. Therefore, understanding these fundamental base pairing stability and specificity provides a foundation for elucidating RNA structure and function relationships, as well as engineering novel RNA-based therapeutics.[9]

[a] Dr. S. Mao, Dr. S.V. Ranganathan, H.-C. Tsai, P. Haruehanroengra, F. Shen, V.A. Valsangkar, Prof. A. Chen, Prof. J. Sheng
Department of Chemistry and The RNA Institute, University at Albany, State University of New York, 1400 Washington Ave. Albany, NY, 12222, USA
E-mail: jsheng@albany.edu
[b] Prof. B. Han, School of Pharmacy, Chengdu University of Traditional Chinese Medicine, Chengdu, 611137, P. R. China
[c] Prof. A.E.A Hassan, Applied Nucleic Acids Research Center, Faculty of Science, Zagazig University, Zagazig, Egypt.

Supporting information for this article is given via a link at the end of the document.

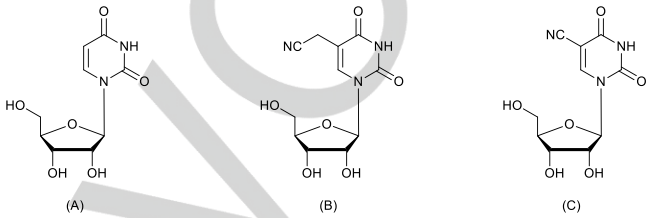

Figure 1. Chemical structure of native U (A), cnm^{5}U (B) and cn^{5}U (C).

Transfer RNA (tRNA), the adaptor molecule linking the messenger RNA codons to the corresponding amino acids during protein synthesis, contains more than 100 chemical modifications that are post-transcriptionally introduced by specific enzymes.[5] In particular, the 'wobble' position 34 of a tRNA, the first anticodon letter, is usually modified by a wide variety of chemical groups for stable structural maintenance, efficient decoding capabilities and accurate amino acids recognition/integration by the translation machinery.[10-15] The 5-cyanomethyluridine (cnm^{5}U) has been discovered recently as a new naturally modified nucleoside (Fig. 1B) at the wobble position of isoleucine tRNAs from mutant *Haloarcula marismortui*.[16] In addition, the cnm^{5}U is also present in the total tRNA of *Methanococcus maripaludis*, indicating its widespread occurrence in euryarchaea tRNAs.[16] This mutant tRNA binds not only to AUA, but also to AUU, another isoleucine codon, as well as to AUG, a methionine codon, resulting in the nonspecific replacement of isoleucine by methionine during the protein expression.[16] This mixed codon recognition pattern implies the low base pairing specificity of this cnm^{5}U residue in RNAs.

Toward our goal of studying detailed working mechanisms of naturally modified RNA nucleotides, we report here the new synthesis of cnm^{5}U contained RNA oligonucleotides and their base pairing stability and specificity studies in the context of RNA duplexes. In addition, many naturally and artificially modified nucleotides have been widely used in developing DNA/RNA oligonucleotides based therapeutics through antisense or RNAi strategies.[17] The introductions of these modified residues can increase the strand stability, facilitate their cellular delivery/transportation and improve their targeting specificity and efficiency. Therefore, inspired by this naturally occurring cnm^{5}U, we also synthesized the 5- cyanouridine (cn^{5}U, Fig. 1C), the close cnm^{5}U analogue with the electron-withdrawing cyano-group directly attached to the uracil, and RNA strands containing this modification. The base pairing stability and specificity comparison in the same RNA duplex indicated that the cnm^{5}U slightly decreases the duplex stability

but retains the base pairing preference with native U. In contrast, the cn^5U dramatically decreases the base pairing stability and specificity between cn^5U:A and other non-canonical cn^5U:G, cn^5U:U and cn^5U:C pairs. The following mechanistic studies by molecular simulation showed that the cn^5U modification does not directly affect the base-pairing of the parent nucleotide, instead, it weakens the neighbouring base-pair in the 5' side of the modification in the RNA duplexes. Consistent with the simulation data, replacing the Watson-Crick AU pair to a mismatched C:U pair in the 5'-neighboring site does not affect the overall duplex stability. Our work implies the significance of electron-withdrawing cyano-group in natural tRNA systems and provides two novel building blocks for constructing RNA based therapeutics.

Results and Discussion

Chemical synthesis of cnm^5U and cn^5U phosphoramidite building blocks and their containing RNA oligonucleotides

Although the synthesis of cnm^5U and cn^5U nucleosides have been achieved,[18-21] more general phosphoramidite building blocks for the solid phase synthesis of oligonucleotides are still required to make different scales of RNA strands. We started the synthesis of cnm^5U from the commercially available 5-methyluridine (**1**, scheme 1), which was fully acetyl-protected, followed by the bromination of 5-methyl group in the presence of NBS and AIBN to give 5-bromomethyluridine (**3**). The cyano-group was subsequently installed by the treatment of TMSCN and TBAF, followed by the deprotection of acetyl groups using ammonium treatment to yield 5-cyanomethyl-uridine (**5**). The 5′- and 2′-hydroxyl groups were selectively protected with dimethoxyltrityl (DMTr) group and *tert*-butyldimethylsilyl (TBDMS) group respectively to obtain the 2′,5′-protected cnm^5U compound (**7**), which is the key intermediate to make the final phosphoramidite building block (**8**) for the oligonucleotides solid phase synthesis.

The synthesis of 5-cyanouridine was started from the regular Vorbrüggen glycosylation of the protected ribofuranose with silylated 5-cyanouracil (**10**, scheme 2) in the presence of Tin (IV) chloride, followed by the deprotection of the benzoyl groups using base treatment. The simultaneous silylation of 3′ and 5′-hydroxyl groups with di-*tert*-butylsilyl (DTBS) ditriflate followed by the 2′-protection with *tert*-butyldimethylsilyl (TBDMS) group gave the silylated 5-cyano uridine (**13**). Subsequently, this compound was selectively desilyated with hydrogen fluoride in pyridine and tritylated with trityl chloride at the 5′ position to generate the key intermediate (**15**), which was converted into the final cn^5U phosphoramidite (**16**) through regular phosphitylation reaction for the solid phase synthesis.

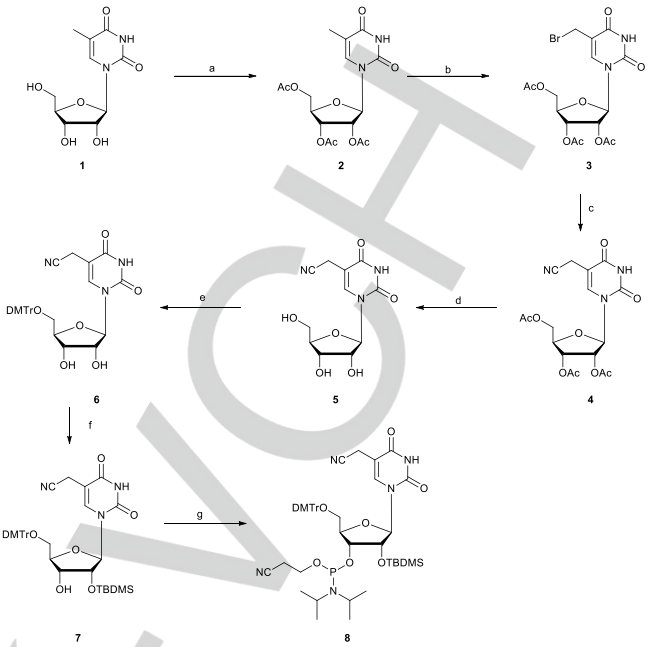

Scheme 1. Synthesis of 5-cyanomethyl-uridine phosphoramidite **8**. Reagents and conditions: (a) Ac_2O, DMAP, pyridine; (b) NBS, AIBN, benzene; (c) TMSCN, TBAF, THF; (d) Ammonia solution, MeOH; (e) DMTrCl, DMAP, pyridine; (f) TBDMSCl, $AgNO_3$, pyridine, THF; (g) (i-Pr_2N)P(Cl)OCH_2CH_2CN, (i-Pr)$_2$NEt, THF.

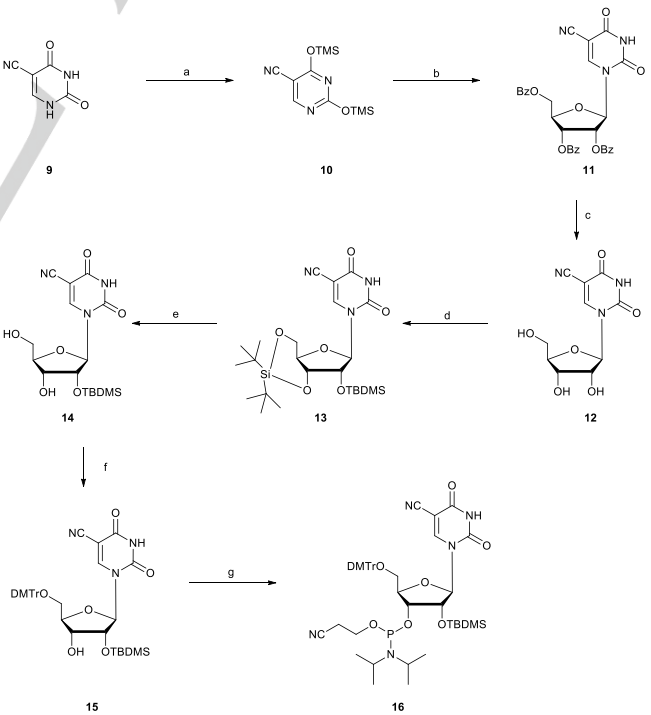

Scheme 2. Synthesis of 5-cyano-uridine phosphoramidite **16**. Reagents and conditions: (a) TMSCl, HMDS; (b) 2,3,5-tri-O-benzoyl-β-D-ribofuranose, $SnCl_4$, 1,2-dichloroethane; (c) NH_3 in methanol; (d) Di-*tert*-butylsilyl ditriflate; TBDMSCl, imidazole, DMF; (e) HF•Py, THF; (f) DMTrCl, pyridine; (g) (i-Pr_2N)P(Cl)OCH_2CH_2CN, (i-Pr)$_2$NEt, CH_2Cl_2.

Table 1. RNA sequences containing cnm^{5}U and cn^{5}U.

Entry	RNA Sequences	Calculated Mass	Measured Mass
ON1	AAUGCcnm^{5}UGCACUG	3832.55	3832.57
ON2	GGACUcnm^{5}UCUGCAG	3848.55	3848.56
ON3	UAGCcnm^{5}UCC	2178.33	2178.02
ON4	UCGcnm^{5}UACGA	2547.39	2547.13
ON5	Gcnm^{5}UACGUAC	2547.39	2547.40
ON6	AAUGCcn^{5}UGCACUG	3818.54	3819.14
ON7	GGACUcn^{5}UCUGCAG	3834.53	3834.54
ON8	UAGCcn^{5}UCC	2164.31	3164.32
ON9	UCGcn^{5}UACGA	2533.37	2533.38

As expected, both of the phosphoramidite building blocks are well compatible with the solid phase synthesis conditions including the trichloroacetic acid (TCA) and oxidative iodine treatments, resulting in very similar coupling yields as the commercially available native phosphoramidite. They are also stable in the basic cleavage from the solid phase beads and the Et_3N•3HF treatment to remove TBDMS protecting groups during the RNA oligonucleotide deprotection and purification. As the demonstration, nine different RNA sequences containing these two modifications have been synthesized and confirmed by ESI- or MALDI-MS spectrum, as shown in Table 1.

Thermal denaturation and base pairing studies of cnm^{5}U and cn^{5}U RNA duplexes

With these RNA strands in hand, we studied the base pairing stability and specificity of both cnm^{5}U and cn^{5}U in RNA duplexes through UV-thermal denaturation experiments. The normalized T_m curves of native and modified RNA duplex, [5′-GGACU**X**CUGCAG-3′ & 3′-CCUGA**Y**GACGUC-5′] with Watson-Crick and other non-canonical base pairs (X pairs with Y) are shown in Supplementary Figure S40. The detailed temperature data are summarized in Table 2. Compared to the native counterparts, both cnm^{5}U and cn^{5}U-modified RNA duplexes showed decreased thermal stability. In the normal U:A paired duplexes (compare entry 1, 5 and 9), the cnm^{5}U decreases the T_m by 3.9 °C, while the cn^{5}U dramatically decreases the T_m by 20.7 °C, corresponding to a ΔG^o reduction of 4.8 and 7.8 kcal/mol respectively. Similarly, the non-canonical base paired (U:G, U:C and U:U) duplexes containing these two modifications also showed significantly lower melting temperatures. With the cnm^{5}U, the T_m drops by 5.3 °C in the U:G mismatched duplex (entry 2 *vs* 6), 3.0 °C in the U:C mismatched one (entry 3 *vs* 7) and 4.2 °C in the U:U mismatched one (entry 4 *vs* 8), corresponding to the ΔG^0 reduction of 4.0, 1.6 and 2.7 kcal/mol respectively. While for the cn^{5}U residue, where the cyano-group is directly attached to the uracil ring, the T_m drops by 16.4 °C in the U:G mismatched duplex (entry 2 *vs* 10), 11.1 °C in the U:C mismatched one (entry 3 *vs* 11) and 15.3 °C in the U:U mismatched one (entry 4 *vs* 12), corresponding to the ΔG^0 reduction of 7.0, 4.1 and 5.9 kcal/mol respectively. These results indicate that the cyano-group on the position 5 of uracil has strong effects on the overall base pairing stability in the context of RNA duplex; and the stronger this electron-withdrawing effect to the uracil ring, the lower the base pairing stability is resulted in. On the other hand, the comparison of the base pairing specificity in each duplex system indicated opposite effects of these two modifications. When directly comparing the T_ms of each Watson-Crick base paired duplex with its own mismatched ones, as shown in the ΔT_m column of Table 2, the cnm^{5}U retains similar base pairing specificity as the native U with slightly increased discrimination between U:A pair and U:G pair by 1.4 °C (entry 2 *vs* 6). However, the cn^{5}U tends to decrease the base pairing discrimination and make the T_m differences much smaller than native counterparts. For example, the T_m of cn^{5}U:C-duplex is only 2 °C lower than the cn^{5}U:A paired one (entry 9 *vs* 11), compared to the native T_m difference of 11.6 °C. More interestingly, the cn^{5}U changes the base pairing preference favouring to G over A by 1.4 °C, corresponding to a ΔG^0 of 0.2 kcal/mol (entry 9 *vs* 10).

Table 2. Duplex stability and base pairing specificity of cnm^{5}U and cn^{5}U in a 12mer RNA duplex [5′-GGACUXCUGCAG-3′ & 3′-CCUGAYGACGUC-5′] (X pairs with Y).

Entry	Base Pairs		T_m (°C)[a]	ΔT_m (°C)[b]	$-\Delta G^0_{37}$ (kcal/mol)[c]
	X	Y			
1	U	A	62.5		16.6
2	U	G	59.6	-2.9	16.0
3	U	C	50.9	-11.6	12.6
4	U	U	53.3	-9.2	14.0
5	cnm^{5}U	A	58.6		11.8
6	cnm^{5}U	G	54.3	-4.3	12.0
7	cnm^{5}U	C	47.9	-10.7	11.0
8	cnm^{5}U	U	49.1	-9.5	11.3
9	cn^{5}U	A	41.8		8.8
10	cn^{5}U	G	43.2	+1.4	9.0
11	cn^{5}U	C	39.8	-2.0	8.5
12	cn^{5}U	U	38.0	-3.8	8.1

[a] The *T*m were measured in sodium phosphate (10 mM, pH 7.0) buffer containing 100 mM NaCl. [b] Δ*T*m values are relative to the RNA duplexes with native and 5-modified U-A pair respectively. [c] Obtained by non-linear curve fitting using Meltwin 3.5.[35]

Molecular simulation of cn^{5}U modified RNA duplexes

To further explore the role of the cn^{5}U modification on lowering the base pairing stability and specificity of RNA duplexes, we performed MD simulations of the duplex in the presence and absence of the modification. Briefly, as outlined in the methods sections, we collected almost a microsecond of simulation data on both the duplexes, and analyzed the trajectories for differences in base-pairing propensities of the nucleotides. We calculated and compared the hydrogen bonding distances (r_{NN}) between paired nucleotides (A/G-N1:U/C-N3, Fig. 2A). The time-series of r_{NN} for the modified base-pair cn5U6:A7 is shown in Fig. 2C and a neighbouring pair U5:A8 shown in Fig. 2B. Interestingly, the behaviour of rNN for the cn^{5}U6:A7 base-pair is unaffected in the presence of the modification, indicating that the cyano- modification does not directly affect the base-pairing propensity of the parent nucleotide. In contrast, we observed a significant difference in the hydrogen bonding distances of the neighbouring base-pair, U5:A8. In the unmodified duplex, this UA base-pair is largely in the paired state, with rare fraying events leading to an "open" state that are short lived (red lines in Fig. 2B). However, in the modified duplex, the fraying events occur much more often, along with a significant increase in the lifetimes of the open state (red lines in Fig. 2B). The time-series r_{NN} data is converted into histograms and are presented in the inset figures, Fig. 2D & 2E. The base-paired or "closed" states produce a strong peak at ~3 Angstroms for both sets of base-pairing nucleotides under consideration. However, the open states in the neighbouring U5:A8 pair produces a weak second peak in the histogram at ~5 Angstroms (seen only in Fig. 2D, prominently in the log-scale). Importantly, the prominence of the second peak increases by ~2 orders of magnitude in the modified duplex compared to the unmodified one, showing a significant increase in the propensity of the neighbouring AU base-pair to adopt an open conformation in the presence of the modification.

The stacking view of two base pairing steps (cn^{5}U6:A7 and U5:A8 in Fig. 2F) with both open and closed states shows more detailed insights into the effect of this cyano-modification on weakening the neighbouring base pairing. The cyano modification can be regarded as a dipole, with roughly equal and opposite charges on the carbon and nitrogen atoms (colored in red and blue, respectively). In the open state, the C2-O2 bond of U5, which can also be treated as a dipole, perfectly aligns with the cyano- group, thereby stabilizing and favouring the adoption of this open state, which in turn disrupts the local structures and might also allow higher hydration of the duplex, therefore leading to lower stability of the overall duplex. In addition, this structural perturbation also decreases the specificity of cn^{5}U6 pairing partners in terms of their contribution to the overall duplex stability.

We further extended the analysis to all the base pairs in this duplex, as presented in Fig. 2G. We defined a cut-off of r_{NN} = 3.2 Angstroms to qualify base-pairing, and compared the unmodified (wild) and modified duplex. It turns out that the modified duplex is overall unaffected by the presence of the modification (including the modified base pair U6:A7), except for the weakening of the U5:A8 base-pair.

To test if the weakening of the base-pair on the 5'-neighbor of the modification site is contributing towards lowering the overall duplex stability, we mutated the A8 residue to C in the complementary strand. Since the base-pairing is already weakened for this position, the mismatch mutation should not cause significant change in the duplex stability. The thermal denaturation experiments of this mutated duplex (A8:U5 to C8:U5) showed very similar T_m. However, mutating 3'-end C:G pair decreases the overall duplex stability by 4.3 °C (Fig. 3 and Table S2), which is consistent with our MD simulation results.

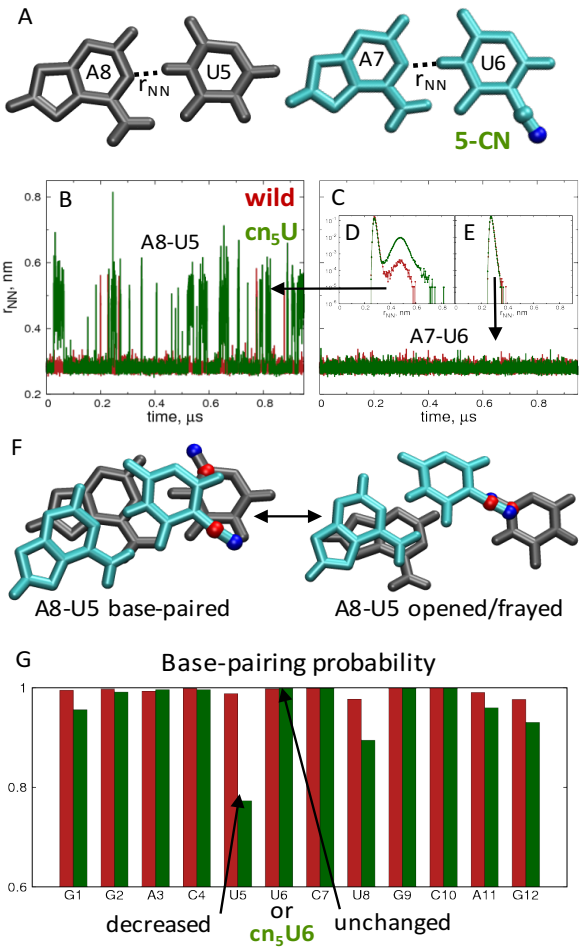

Figure 2. MD Simulation results for the RNA duplex [5′-GGACUXCUGCAG-3′ & 3′-CCUGAYGACGUC-5′], where X represents either modified or native U6, Y represents the complimentary base A7. Nucleotides numbering is from 5'-end in both strands. (A) Base-pairing schemes for modified and unmodified A:U bases. Licorice representation was used for the bases, with the modification highlighted in CPK. (B) & (C) Time-series data, r_{NN} for A8-U5 and A7-U6 base-pairs, respectively. Unmodified duplex (wild) is shown in red, and the modified duplex is shown in green. (D) & (E) Histograms form the time-series data in (B) & (C), respectively. (F) Simulation snapshots, showing the dipole alignment of the modification in the open state. Same color coding as (A), except for the two dipoles, highlighted in red and blue. (G) Base-pairing probabilities for the entire duplex (red--wild; green--modified)..

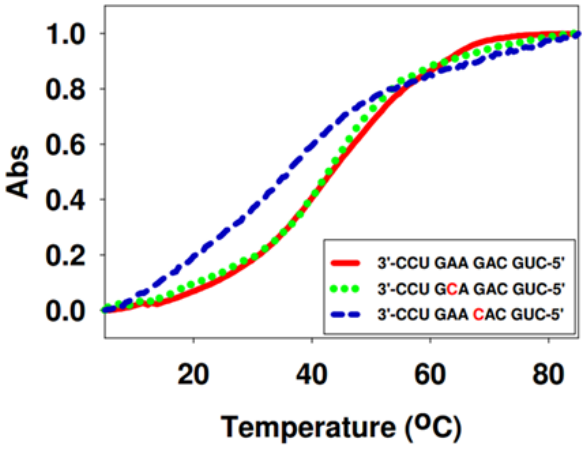

Figure 3. Normalized UV-melting curves of controlled RNA duplexes. The cn^{5}U modified sequence 5'-GGACU**cn^{5}U**CUGCAG-3' pairs with 3'-CCUGA**A**GACGUC-5' strand (in red solid line); with 3'-CCUG**C**A**A**GAC GUC-5' strand (in green dotted line); and with 3'-CCUGA**A**CACGUC-5' strand (blue dash line).

Conclusions

In summary, we have synthesized the cnm^{5}U and cn^{5}U phosphoramidites and a series of RNA oligonucleotides containing these two residues. Our base pairing stability and specificity studies showed that the 5-cyano-group on the uracil has strong effects on its base pairing stability. While the cnm^{5}U retains the similar base pairing specificity between U:A and other non-canonical pairs as native uridine, the cn^{5}U dramatically decrease the discrimination between these base pairs. More interestingly, the cn^{5}U:G pair shows higher thermal stability than the cn^{5}U:A pair in the context of RNA duplex, implying that the cn^{5}U might slightly prefer to recognize G over A. The molecular simulation studies results showed that the cn^{5}U modification does not directly affect the base-pairing of the parent nucleotide, instead, it weakens the neighbouring base-pair in the 5' side of the modification in the RNA duplexes. Consistent with the simulation results, replacing the Watson-Crick A:U pair to a mismatched C:U pair in the 5'-neighboring site does not affect the overall duplex stability. Although it has not been discovered in the natural RNA systems, our results indicate that the cn^{5}U residue might be used by certain biological systems like virus RNA to increase the base pairing diversify and induce higher rates of gene mutation, even though it decreases the overall base pairing stability. In addition, this work provides two novel building blocks for constructing RNA-based therapeutics.

Experimental Section

Materials and general procedures of synthesis

Anhydrous solvents were used and redistilled using standard procedures. All solid reagents were dried under a high vacuum line prior to use. Air sensitive reactions were carried out under argon. RNase-free water, tips and tubes were used for RNA purification, crystallization and thermodynamic studies. Analytical TLC plates pre-coated with silica gel F254 (Dynamic Adsorbents) were used for monitoring reactions and visualized by UV light. Flash column chromatography was performed using silica gel (32-63 μm). All ^{1}H, ^{13}C and ^{31}P NMR spectra were recorded on a Brucker 400 spectrometer. Chemical shift values are in ppm. ^{13}C NMR signals were determined by using APT technique. High-resolution MS were achieved by ESI at University at Albany, SUNY.

Synthesis of cn^{5}U and cnm^{5}U phosphoramidites

1-(2',3',5'-tri-O-acetyl-beta-D-ribofuranosyl)-5-methyluridine **2**.[22] To a solution of compound **1** (200 mg, 0.77 mmol) in pyridine (8 mL) was added DMAP (19 mg, 0.155 mmol) and Ac_2O (0.73 mL, 7.75 mmol) at room temperature. The mixture was stirred for 12 h. After removing the solvent, The residue was purified by silica gel column chromatography to give compound **2** (266 mg, 90%) as a light brown oil. TLC R_f = 0.4 (50% EtOAc in CH_2Cl_2). ^{1}H-NMR (400 MHz, $CDCl_3$): δ 7.18 (s, 1H), 6.07 (d, *J* = 4.8Hz, 1H), 5.33-5.30 (m, 2H), 4.36-4.33 (m, 3H), 2.17 (s, 3H), 2.13 (s, 3H), 2.10 (s, 3H), 1.95 (s, 3H).

1-(2',3',5'-tri-O-acetyl-beta-D-ribofuranosyl)-5-bromomethyluridine **3**.[23] To a solution of compound **2** (150 mg, 0.39 mmol) in benzene (4 mL) was added NBS (90.31 mg, 0.51 mmol) and AIBN (8.33 mg, 0.05 mmol). The reaction was heated at 80 °C for 4 h. After removing the solvent, the residue was purified by silica gel column chromatography to give compound **3** as a light brown solid (140 mg, 80%). TLC R_f = 0.5 (50% EtOAc in CH_2Cl_2). ^{1}H-NMR (400 MHz, $CDCl_3$): δ 7.65 (s, 1H), 6.03 (d, *J* = 4.8 Hz, 1H), 5.39-5.27 (m, 2H), 4.42-4.22 (m, 5H), 2.17 (s, 3H), 2.12 (s, 3H), 2.09 (s, 3H).

1-(2',3',5'-tri-O-acetyl-beta-D-ribofuranosyl)-5-cyanomethyluridine **4**. To a solution of compound **3** (180.8 mg, 0.39 mmol) in THF (4 mL) was added TMSCN (0.24 mL, 1.95 mmol) and TBAF (1.95 mL, 1.95 mmol) at room temperature. The reaction was stirred for 1.5 h. The reaction was quenched with water and extracted with ethyl acetate. After drying the organic layer over Na_2SO_4 and evaporation. The residue was purified by silica gel column chromatography to give compound **4** (111.8 mg, 70%) as a light brown solid. TLC R_f = 0.4 (50% EtOAc in CH_2Cl_2). ^{1}H-NMR (400 MHz, $CDCl_3$): δ 7.58 (s, 1H), 6.02-6.00 (m, 1H), 5.36-5.29 (m, 2H), 4.40-4.26 (m, 3H), 3.44 (s, 2H), 2.12 (s, 3H), 2.09 (s, 3H), 2.05 (s, 3H). HRMS (ESI-TOF) $[M+Na]^+$ = 432.1050 (calc. 432.1121). Chemical formula: $C_{17}H_{19}N_3O_9$.

5-cyanomethyluridine **5**.[18] To a solution of compound **4** (200 mg, 0.49 mmol) in MeOH (4 mL) was added the ammonia solution (0.19 mL, 2.93 mmol) at room temperature, the resulting solution was stirred at room temperature for 15 h. Solvent was removed by repeat evaporation with readdition of MeOH to remove all ammonia. The residue was purified by silica gel column chromatography to give compound **5** (125 mg, 90%) as a white solid. TLC R_f = 0.3 (20% MeOH in CH_2Cl_2). ^{1}H-NMR (400MHz, MeOD): δ 8.16 (s, 1H), 5.90 (m, 1H), 4.17 (m, 2H), 4.02-3.99 (m, 1H), 3.89-3.83 (m, 1H), 3.77-3.74 (m, 1H), 3.48 (s, 2H). HRMS (ESI-TOF) $[M+H]^+$ = 284.0868 (calc. 284.0883). Chemical formula: $C_{11}H_{13}N_3O_6$.

1-(5'-O-4,4'-dimethoxytrityl-beta-D-ribofuranosyl)-5-cyanomethyluridine **6**. Compound **5** (200 mg, 0.706 mmol) evaporated with pyridine three times and then dissolved in pyridine (7 mL). DMTrCl (286.99 mg, 0.847 mmol) was added. The reaction was stirred at room temperature in the dark for 12 h. The reaction was quenched with methanol (1 mL). After removing the solvent and the residue was purified by silica gel column chromatography to give compound **6** (400 mg, 97%) as a white solid.

TLC R_f = 0.4 (10% MeOH in CH_2Cl_2). ^{1}H-NMR (400 MHz, $CDCl_3$): δ 7.98 (s, 1H), 7.39-7.37 (m, 2H), 7.34-7.25 (m, 7H), 6.87-6.84 (m, 4H), 5.96 (d, *J* = 3.2 Hz, 1H). 4.48-4.32 (m, 2H), 4.20-4.18 (m, 1H), 3.78 (s, 6H), 3.56-3.53 (m, 1H), 3.47-3.44 (m, 1H), 2.59 (d, *J* = 17.2 Hz, 1H), 2.46 (d, *J* = 17.2 Hz, 1H). ^{13}C NMR (100 MHz, $CDCl_3$) δ162.4, 158.8, 158.8, 150.8, 144.2, 139.3, 135.1, 135.0, 130.1, 130.1, 128.2, 128.1, 127.4, 127.4, 113.4, 105.2, 87.2, 83.9, 55.2, 15.0. HRMS (ESI-TOF) $[M+Na]^+$ = 608.2024 (calc. 608.2009). Chemical formula: $C_{32}H_{31}N_3O_8$.

1-(2'-O-tert-butyldimethylsilyl-5'-O-4,4'-dimethoxytrityl-beta-D-ribofuranosyl)-5-cyanomethyluridine **7**. To a solution of compound **6** (200 mg, 0.342 mmol) in THF (3.5 mL) was added pyridine (81 µL) and $AgNO_3$ (92.75 mg, 0.546 mmol). The reaction was stirred at room temperature in the dark for 30 min. Then, TBDMSCl (90.28 mg, 0.6 mmol) was added and the resulting solution was stirred at room temperature in the dark for another 12 h. After removing the solvent and the residue was purified by silica gel column chromatography to give compound **7** (100 mg, 42%) as a white solid. TLC R_f = 0.7 (5% MeOH in CH_2Cl_2). ^{1}H-NMR (400 MHz, $CDCl_3$): δ 7.98 (s, 1H), 7.39-7.25 (m, 9H), 6.89-6.86 (m, 4H), 6.0 (d, *J* = 3.2 Hz, 1H), 4.47-4.44 (m, 1H), 4.37-4.35 (m, 1H), 3.81 (s, 6H), 3.57-3.36 (m, 2H), 2.53 (d, *J* = 17.2 Hz, 1H), 2.28 (d, *J* = 17.2 Hz, 1H), 0.94 (s, 9H), 0.18 (s, 6H). ^{13}C NMR (100 MHz, $CDCl_3$) δ 159.0, 158.9, 149.8, 144.1, 138.7, 134.9, 134.7, 130.2, 130.1, 129.1, 128.1, 127.5, 116.1, 113.5, 113.3, 113.2, 105.3, 88.7, 87.3, 83.8, 62.8, 55.2, 25.6, 18.0, -4.7, -5.2. HRMS (ESI-TOF) $[M+H]^+$ = 700.2960 (calc. 700.3054). Chemical formula: $C_{38}H_{45}N_3O_8Si$.

1-[2'-O-tert-butyldimethylsilyl-3'-O-(2-cyanoethyl-N,N-diisopropylamino)phosphoramidite-5'-O-(4,4'-dimethoxytrityl-beta-D-ribofuranosyl)]-5-cyanomethyluridine **8**. To a solution of compound **7** (70 mg, 0.1 mmol) in THF (1 mL) was added DIPEA (0.14 mL, 0.8 mmol) and stirred at room temperature for 30 min. $(i\text{-Pr})_2NPClOCH_2CH_2CN$ (0.05 mL, 0.2 mmol) was added and the mixture was stirred at room temperature for 12 h. The reaction was quenched with water and extracted with DCM. The organic layer was dried by anhydrous sodium sulfate, filtered and evaporated under reduced pressure. The residue was purified by flash silica gel chromatography to give compound **8** (73 mg, 0.08 mmol, 80% yield) as a white solid. TLC R_f = 0.7 (5% MeOH in CH_2Cl_2). ^{1}H NMR (400MHz, $CDCl_3$) δ 8.06-7.94 (m, 1H), 7.44-7.26 (m, 9H), 6.89-6.85 (m, 4H), 6.18-5.94 (m, 1H), 4.52-4.44 (m, 1H), 4.39-4.29 (m, 2H), 4.29-4.14 (m, 1H), 3.98-3.90 (m, 1H), 3.57-3.50 (m, 1H), 3.44-3.32 (m, 1H), 2.75-2.54 (m, 3H), 2.46-2.40 (m, 1H), 1.17 (s, 12H), 0.91 (s, 9H), 0.16 (s, 6H). ^{31}P NMR ($CDCl_3$) δ 149.89, 149.57. HRMS (ESI-TOF) $[M+NH_4]^+$ = 900.4235 (calc. 900.4054). Chemical formula: $C_{47}H_{62}N_5O_9PSi$.

1-(2',3',5'-tri-O-benzoate-beta-D-ribofuranosyl)-5-cyanouridine **11**. To a solution of compound **9** (8.22 g, 60 mmol) in hexamethyldisilazane (HMDS, 500 mL) was added trimethylsiylchloride (TMSCl, 15.2 mL, 120 mmol). The mixture was stirred at 130 °C for 20 h until the mixture turned clear. Then, the solution evaporated to remove excess HMDS and compound **10** was obtained and immediately used without further purification. At room temperature, to a solution of compound **10** and 2,3,5-tri-O-benzoyl-β-D-ribofuranose (33.26 g, 66 mmol) in 1,2-dichloroethane (DCE, 500 mL) was added $SnCl_4$ (7.8 mL, 66 mmol) slowly at 0 °C. After 30 min, the reaction was brought to room temperature and continued for another 2 h. Then, the reaction was quenched with saturated $NaHCO_3$ aqueous solution (500 mL) at 0 °C and extracted with DCM (3 x 500 mL). The organic layer was dried by anhydrous sodium sulfate, filtered and evaporated under reduced pressure. The residue was purified by silica gel chromatography to give compound **11** (30 g, 51.64 mmol, 86% yield) as a white solid. TLC R_f = 0.6 (10% MeOH in CH_2Cl_2). ^{1}H NMR (400MHz, $CDCl_3$) δ 8.14 (s, 1H), 8.10-7.88 (m, 6H), 7.64-7.33 (m, 9H), 6.23 (d, *J* = 5.2 Hz), 5.86 (m, 1H), 5.72-5.69 (m, 1H), 4.80 (m, 3H). HRMS (ESI-TOF) $[M+NH_4]^+$ = 599.1830 (calc. 599.1778). Chemical formula: $C_{31}H_{23}N_3O_9$.

5-cyanouridine **12**.[21] Compound **11** (5.81 g, 10 mmol) was dissolved in 50 mL of 7N NH_3/MeOH at room temperature, and stirred for 12 h. Solvent was removed by repeat evaporation with readdition of MeOH to remove all ammonia. The residue was purified by silica gel chromatography to give compound **12** (1.80 g, 6.69 mmol, 67% yield) as a white solid. TLC R_f = 0.4 (25% MeOH in CH_2Cl_2). ^{1}H NMR (400 MHz, MeOD) δ 9.02 (s, 1H), 5.83 (d, *J* = 2.8 Hz, 1H), 4.21-4.16 (m, 2H), 4.07-4.03 (m, 1H), 3.95 (dd, *J* = 2.4 Hz, 12.4 Hz, 1H), 3.77 (dd, *J* = 2.4 Hz, 12.4 Hz, 1H). HRMS (ESI-TOF) $[M+Na]^+$ = 292.0564 (calc. 292.0546). Chemical formula: $C_{10}H_{11}N_3O_6$.

1-(2'-O-tert-butyldimethylsilyl-3',5'-O-di-tert-butylsilylene-beta-D-ribofuranosyl)-5-cyanouridine **13**. Compound **12** (1.40 g, 5.2 mmol) was suspended in DMF (20 mL) and cooled to 0 °C. Then di-*tert*-butylsilyl bis(trifluoromethanesulfonate) (2.4 mL, 6.24 mmol) was added dropwise and the resulting solution was stirred at 0 °C for 1 h. Subsequently, imidazole (2.04 g, 26 mmol) was added and the mixture was warmed to room temperature at which TBDMS-Cl (1.1 g, 6.24 mmol) was added. The reaction was allowed to proceed at 60 °C for 2 h. Then, the reaction was quenched with water (50 mL) and extracted with DCM (3 x 50 mL). The organic layer was dried by anhydrous sodium sulfate, filtered and evaporated under reduced pressure. The residue was purified by silica gel chromatography to give compound **13** (2.40 g, 4.59 mmol, 88% yield) as a white solid. TLC R_f = 0.7 (30% ethyl acetate in hexane). ^{1}H NMR (400MHz, $CDCl_3$) δ 7.91 (s, 1H), 5.64 (s, 1H), 4.58-4.53 (m, 1H), 4.30-4.23 (m, 2H), 4.03-3.98 (m, 1H), 3.78-3.73 (m, 1H), 1.06 (s, 9H), 1.03 (s, 9H), 0.94 (s, 9H), 0.19 (s, 3H), 0.15 (s, 3H). ^{13}C NMR (100 MHz, $CDCl_3$) δ 159.52, 159.47, 148.2, 147.5, 112.8, 94.1, 90.1, 75.3, 75.1, 22.6, 20.3, 18.1, -4.1, -4.3, -5.0, -5.2. HRMS (ESI-TOF) $[M+H]^+$ = 524.2641 (calc. 524.2612). Chemical formula: $C_{24}H_{41}N_3O_6Si_2$.

1-(2'-O-tert-butyldimethylsilyl-beta-D-ribofuranosyl)-5-cyanouridine **14**. To a solution of compound **13** (2.10 g, 4.00 mmol) in tetrahydrofuran (20 mL) at 0 °C was added a solution of hydrogen fluoride-pyridine complex (hydrogen fluoride ~70%, pyridine ~30%) (0.4 mL) in pyridine (2 mL). After 1 h at 0 °C the reaction was complete and pyridine (15 mL) was added. The reaction mixture was washed with saturated $NaHCO_3$, dried over Na_2SO_4 and evaporated. The residue was purified by silica gel chromatography to give compound **14** (1.10 g, 2.87 mmol, 75% yield) as a white solid. TLC R_f = 0.4 (10% MeOH in CH_2Cl_2). ^{1}H NMR (400MHz, CD_3OD) δ 9.12 (s, 1H), 5.76 (s, 1H), 4.27 (m, 1H), 4.15-4.04 (m, 2H), 4.01-3.97 (m, 1H), 3.81-3.77 (m, 1H), 0.94 (s, 9H), 0.15 (d, 6H). ^{13}C NMR (100 MHz, $CDCl_3$) δ 160.61, 160.60, 149.7, 149, 4, 149, 1, 113.2, 90.8, 88.3, 76.7, 76.4, 17.6, -6.0. HRMS (ESI-TOF) $[M+Na]^+$ = 406.1411 (calc.406.1410). Chemical formula: $C_{16}H_{25}N_3O_6Si$.

1-(2'-O-tert-butyldimethylsilyl-5'-O-4,4'-dimethoxytrityl-beta-D-ribofuranosyl)-5-cyanouridine **15**. To a solution of compound **14** (766 mg, 2 mmol) in dry pyridine (10 mL) was added 4,4'-Dimethoxytrityl chloride (812 mg, 2.4 mmol) under Ar. The resulting solution was stirred at room temperature for 12 h. The reaction was quenched with methanol (1 mL) and stirred for another 5 min. The reaction mixture was then concentrated to dryness under vacuum. The residue was purified by silica gel chromatography to give compound **15** (1.20 g, 1.75 mmol, 73% yield) as a white solid. TLC R_f = 0.5 (50% ethyl acetate in hexane). ^{1}H NMR (400MHz, $CDCl_3$) δ 8.42 (s, 1H), 7.42-7.39 (m, 2H), 7.35-7.24 (m, 7H), 6.89-6.86 (m, 4H), 5.90 (d, *J* = 3.2 Hz, 1H), 4.50 (m, 1H), 4.43 (m, 1H), 4.22 (m, 1H), 3.80 (s, 6H), 3.58-3.55 (m, 1H), 3.42-3.35 (m, 1H), 0.95 (s, 9H), 0.19 (d, 6H). ^{13}C NMR (100 MHz, CDCl3) δ 159.1, 158.8, 158.7, 148.6, 147,8, 147.68, 147,67, 144.0, 135.1, 134.7, 113.6, 113.4, 111.6, 90.8, 89.8, 89.76, 87.4, 80.3, 70.7, 18.0, -4.6, -5.1. HRMS (ESI-

TOF) $[M+Na]^+$= 708.2716 (calc. 708.2717). Chemical formula: $C_{37}H_{43}N_3O_8Si$.

1-[2'-O-tert-butyldimethylsilyl-3'-O-(2-cyanoethyl-N,N-diisopropylamino)phosphoramidite-5'-O-(4,4'-dimethoxytrityl-beta-D-ribofuranosyl)]-5-cyanouridine **16**. To a solution of compound **15** (685 mg, 1 mmol) in dry tetrahydrofuran (8 mL) was added N,N-di-*iso*-propylethylamine (0.7 mL) and 2-cyanoethyl N,N-diisopropylchlorophosphoramidite (0.5 mL). The resulting solution was stirred at room temperature for 12 h under argon gas. The reaction was quenched with water and extracted with ethyl acetate. After drying the organic layer over Na_2SO_4 and evaporation. The residue was purified by flash silica gel chromatography to give compound **16** (800 mg, 0.9 mmol, 90% yield) as a white solid. TLC R_f = 0.5 (50% ethyl acetate in hexane). ^{1}H NMR (400MHz, $CDCl_3$) δ 8.43-8.38 (m, 1H), 7.49-7.25 (m, 9H), 6.90-6.87 (m, 4H), 5.92-5.77 (m, 1H), 4.61 (m, 1H), 4.44-4.33 (m, 2H), 3.80 (s, 6H), 3.63-3.46 (m, 5H), 2.69-2.65 (m, 1H), 2.47 (m, 1H), 1.17 (s, 12H), 0.92 (s, 9H), 0.18 (s, 6H). ^{31}P NMR ($CDCl_3$) δ 150.09, 149.63. HRMS (ESI-TOF) $[M+H]^+$ = 886.4015 (calc. 886.3976). Chemical formula: $C_{46}H_{60}N_5O_9PSi$.

Synthesis, HPLC and characterization of RNA oligonucleotides

All oligonucleotides were chemically synthesized at 1.0 µmol scales by solid phase synthesis using the Oligo-800 synthesizer. The cnm^{5}U and cn^{5}U-phosphoramidite was dissolved in acetonitrile to a concentration of 0.07 M. I_2 (0.02 M) in THF/Py/H_2O solution was used as an oxidizing reagent. Coupling was carried out using 5-ethylthio-1H-tetrazole solution (0.25 M) in acetonitrile for 12-min, for both native and modifed phosphoramidites. About 3% trichloroacetic acid in methylene chloride was used for the 5'-detritylation. Synthesis was performed on control-pore glass (CPG-500) immobilized with the appropriate nucleoside through a succinate linker. All the reagents used are standard solutions obtained from ChemGenes Corporation. All canonical rA, U, rG and rC phosphoramidites are purchased from ChemGenes Corporation. Phosphoramidite rA is N-Bz protected, rC is N-Ac protected and rG is N-^{t}Bu protected. The oligonucleotide was prepared in DMTr off form. After synthesis, the oligos were cleaved from the solid support and fully deprotected with concentrated ammonium solution at room temperature for 14 h. The solution was evaporated to dryness by Speed-Vac concentrator. The solid was dissolved in 100 µL and was desilylated using a triethylamine trihydrogen fluoride (Et_3N•3HF) solution at 65 °C for 2.5 h. Cooled down to room temperature the RNA was precipitated by adding 0.025 mL of 3 M sodium acetate and 1 mL of ethanol. The solution was cooled to -80 °C for 1 h before the RNA was recovered by centrifugation and finally dried under vacuum.

The oligonucleotides were purified by reverse phase HPLC using a Zorbax SB-C18 column at a flow rate of 1 mL/min. Buffer A was 20 mM Tris-HCl, pH 8.0; buffer B 1.25 M NaCl in 20 mM Tris-HCl, pH 8.0. A linear gradient from 100% buffer A to 70% buffer B in 20 min was used to elute the oligos. The analysis was carried out by using the same type of analytical column with the same eluent gradient. All the modified-oligos were checked by high-resolution MS.

UV-melting temperature (*T*m) study

Solutions of the duplex RNAs (1.5 µM) were prepared by dissolving the purified RNAs in sodium phosphate (10 mM, pH 7.0) buffer containing 100 mM NaCl. The solutions were heated to 95 °C for 5 min, then cooled down slowly to room temperature, and stored at 4 °C for 2 h before Tm measurement. Thermal denaturation was performed in a Cary 300 UV-Visible Spectrophotometer with a temperature controller. The temperature reported is the block temperature. Each denaturizing curves were acquired at 260 nm by heating and cooling from 5 to 80 °C for four times in a rate of 0.5 °C/min. All the melting curves were repeated for at least four times. The thermodynamic parameter of each strand was obtained by fitting the melting curves in the Meltwin software.

Simulation method

We performed molecular dynamics (MD) simulations of the RNA duplex in the presence and absence of the modification. To do so, we developed AMBER-type [24] force-field parameters for the modified uridine in the following way. We performed Restrained Electrostatic Potential (RESP) fit on the RED server [25] at Hartree-Fock (HF) level theory with 6-31G* basis-set to obtain partial charges of the modified base.[26] The bonded interactions were obtained from General AMBER Force-field (GAFF), and the non-bonded interactions from AMBER99 force-field with Chen-Garcia corrections.[27] The rest of the duplex also employed AMBER99 force-filed with Chen-Garcia corrections for the base, and Cheatham-Bergonzo[28] corrections for the backbone atoms.

The duplex was constructed as an A-form helix using the make-na server, employing the NAB suite of AMBER. The modification is introduced in the duplex and minimized in vacuum before introducing in the 0.1M NaCl solution. The simulation system was a 6 x 6 x 6 nm^3 3D periodic box containing the RNA duplex, 6763 water molecules, 35 Na^+ and 13 Cl^- ions. TIP4P-Ew[29] model was used for the water molecules, and Joung & Cheatham parameters[30] for the ions.

All simulations were performed using Gromacs-2016 simulation package. The simulations incorporated leap-frog algorithm with a time-step of 1 fs. The systems were studied in NPT ensemble by maintaining the temperature at 300 K and the pressure at 1 bar using a V-rescale thermostat[31] and Parrinello-Rahman[32], respectively. The electrostatic interactions were calculated using Particle Mesh Ewald (PME)[33], with a real space cut-off of 1.2 nm. LJ interactions were also cut-off at 1.2 nm. LINCS algorithm[34] was used to constrain h-bonds. The production runs consisted of ten 100 ns runs starting from an equilibrated system, totalling a microsecond of data to analyze for each of the duplexes. The configurations of the RNA were stored at 2 ps intervals for further analysis.

Acknowledgements

We are grateful to NSF (MCB-1715234) and the University at Albany, State University of New York for the financial support. We thank Prof. Maksim Royzen, Prof. Daniele Fabris, Dr. Reza Nemti, Cen Chen, Muhan He and Thomas Kenderdine for their help in MS-Spec analysis.

Conflicts of interest

There are no conflicts to declare.

Keywords: RNA modification • base pair • phosphoramidites • solid-phase synthesis • oligonucleotides

[1] M. J. Fedor, *Annu. Rev. Biophys.* **2009**, *38*, 271-299.
[2] J. A. Doudna, J. R. Lorsch, *Nat. Struct. Mol. Biol.* **2005**, *12*, 395-402.

[3] T. M. Henkin, *Gene. Dev.* **2008**, *22*, 3383-3390.
[4] A. Roth, R. R. Breaker, *Annu. Rev. Biochem.* **2009**, *78*, 305-334.
[5] P. Boccaletto, M. A. Machnicka, E. Purta, P. Piatkowski, B. Baginski, T. K. Wirecki, V. de Crécy-Lagard, R. Ross, P. A. Limbach, A. Kotter, M. Helm, J. M. Bujnicki, *Nucleic Acids Res.* **2018**, *46*, D303-D307.
[6] W. A. Cantara, P. F. Crain, J. Rozenski, J. A. McCloskey, K. A. Harris, X. Zhang, F. A. Vendeix, D. Fabris, P. F. Agris, *Nucleic Acids Res.* **2011**, *39*, D195-201.
[7] C. J. Lewis, T. Pan, A. Kalsotra, *Nat. Rev. Mol. Cell Bio.* **2017**, *18*, 202-210.
[8] N. B. Leontis, J. Stombaugh, E. Westhof, *Nucleic Acids Res.* **2002**, *30*, 3497-3531.
[9] P. H. Hagedorn, B. R. Hansen, T. Koch, M. Lindow, *Nucleic Acids Res.* **2017**, *45*, 2262-2282.
[10] H. Grosjean, *DNA and RNA Modification Enzymes: Structure, Mechanism, Function and Evolution*, Landes Bioscience, Austin, **2009**, pp. 1-18.
[11] P. F. Agris, F. A. Vendeix, W. D. Graham, *J. Mol. Biol.* **2007**, *366*, 1-13.
[12] S. Yokoyama, S. Nishimura, *tRNA: Structure, Biosynthesis, and Function*, American Society for Microbiology, Washington, D. C., **1995**, pp. 207-224.
[13] G. R. Björk, *tRNA: Structure, Biosynthesis, and Function*, American Society for Microbiology, Washington, D. C., **1995**, pp. 165-205.
[14] T. Suzuki, *Topics in Current Genetics, Vol. 12*, Springer-Verlag, Berlin, **2005**, pp. 23-69.
[15] M. Helm, J. D. Alfonzo, *Chem. Biol.* **2014**, 21, 174-185.
[16] D. Mandal, C. Köhrer, D. Su, I. R. Babu, C. T. Y. Chan, Y. Liu, D. Söll, P. Blum, M. Kuwahara, P. C. Dedon, U. L. Rajbhandary, *RNA* **2014**, *20*, 177-188.
[17] M. Egli, P. S. Pallan, *Annu. Rev. Biophys. Biomol. Struct.* **2007**, 36, 281-305.
[18] K. Bartosik, E. Sochacka, G. Leszczynska, *Org. Biomol. Chem.* **2017**, *15*, 2097-2103.
[19] G. T. Badman, C. B. Reese, *J. Chem. Soc., Chem. Commun.* **1987**, 1732-1734.
[20] K. Ikeda, S. Tanaka, Y. Mizuno, *Chem. Pharm. Bull.* **1975**, *23,* 2958-2964.
[21] M. E. Meza-Avina, L. Wei, Y. Liu, E. Poduch, A. M. Bello, R. K. Mishra, E. F. Pai, L. P. Kotra, *Bioorg. Med. Chem.* **2010**, *18*, 4032-4041.
[22] K. Takenuki, H. Itoh, A. Matsuda, T. Ueda, *Chem. Pharm. Bull.* **1990**, *38*, 2947-2952.
[23] M. Munzel, D. Globisch, T. Bruckl, M. Wagner, V. Welzmiller, S. Michalakis, M. Muller, M. Biel, T. Carell, *Angew. Chem. Int. Ed.* **2010**, *49*, 5375-5377.
[24] W. D. Cornell, P. Cieplak, C. I. Bayly, I. R. Gould, K. M. Merz, D. M. Ferguson, D. C. Spellmeyer, T. Fox, J. W. Caldwell, P. A. Kollman, *J. Am. Chem. Soc.* **1995**, *117*, 5179-5197.
[25] F. Y. Dupradeau, A. Pigache, T. Zaffran, C. Savineau, R. Lelong, N. Grivel, D. Lelong, W. Rosanski, P. Cieplak, *Phys. Chem. Chem. Phys.* **2010**, *12*, 7821-7839.
[26] W. D. Cornell, P. Cieplak, C. I. Bayly, P. A. Kollman, *J. Am. Chem. Soc.* **1993**, *115*, 9620-9631.
[27] A. A. Chen, A. E. García, *Proc. Natl. Acad. Sci. U. S. A.* **2013**, *110*, 16820-16825.
[28] C. Bergonzo, T. E. Cheatham III, *J. Chem. Theory Comput.* **2015**, 11, 3969-3972.
[29] C. Vega, J. L. Abascal, I. Nezbeda, *J. Chem. Phys.* **2006**, *125*, 34503.
[30] I. S. Joung, T. E. Cheatham III, *J. Phys. Chem. B* **2008**, *112*, 9020-9041.
[31] G. Bussi, D. Donadio, M. Parrinello, *J. Chem. Phys.* **2007**, *126*, 014101.
[32] H. J. C. Berendsen, J. P. M. Postma, W. F. van Gunsteren, A. DiNola, J. R. Haak, *J. Chem. Phys.* **1984**, *81*, 3684-3690.
[33] T. A. Darden, L. G. Pedersen, *Environ. Health Perspect.* **1993**, *101*, 410-412.
[34] B. Hess, B. Bekker, H. J. C. Berendsen, J. G. E. M. Fraaije, *J. Comput. Chem.* **1997**, *18*, 1463-1472.
[35] J. A. McDowell, D. H. Turner, *Biochemistry* **1996**, *35*, 14077-14089.

Entry for the Table of Contents

FULL PAPER

5-cyanomethyluridine (cnm^{5}U) and 5-cyanouridine (cn^{5}U) are synthesized and incorporated into RNA oligonucleotides. The biophysical and structural studies indicate that cnm^{5}U slightly decreases the duplex stability but retains base pairing selectivity. In contrast, cn^{5}U dramatically decreases both base pairing stability and specificity through neighbouring disruption in RNA duplexes.

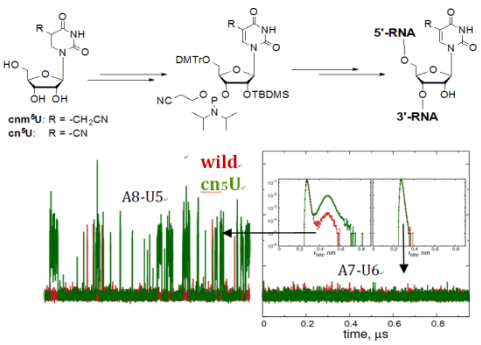

Cyano-modification on Uridine Decrease the Base Pairing Stability and Specificity through Neighbouring Disruption in RNA Duplex

*Song Mao, Srivathsan V. Ranganathan, Hsu-Chun Tsai, Phensinee Haruehanroengra, Fusheng Shen, Vibhav A. Valsangkar, Bo Han, Abdalla E. A. Hassan, Alan Chen and Jia Sheng**

Page No. – Page No.